Article

Preparation of Galangin self-microemulsion Drug Delivery System and Evaluation of Its Pharmacokinetics In Vivo and Antioxidant Activity In Vitro

Hao Lu , Xiwen Chen , and Hanlin Xu ,*

Hubei University of Chinese medicine; luhao@hbtcm.edu.cn
Hubei University of Chinese medicine; 1831800112@stmail.hbtcm.edu.cn
* Correspondence: xhl@hbtcm.edu.cn; Tel.: (+86-027-68890101)

Abstract: Galangin(Gal) is a natural active flavonoid compound separated from the roots and rhizomes of Alpinia ofcinarum Hance. Modern pharmacological studies have shown that Gal has a variety of biological activities such as anti-tumor, anti-fungal, anti-bacterial, anti-inflammatory, anti-ischemic stroke, suppressing vitiligo and Alzheimer's disease, etc. The purpose of this research was to prepare a galangin self-microemulsion drug delivery system (Gal-SMEDDS) and compare its anti-oxidant activity and pharmacokinetics with free Gal.The average particle size of the prepared Gal-SMEDDS was approximately 21.33 nm, the polydispersity index was 0.096, the zeta potential was -4.09 mV, and the entrapment efficiency was 96.74%. Compared with free Gal, the release of Gal-SMEDDS was improved in vitro release experiment. Cell experiments showed that Gal had obvious anti-oxidation effect, and the effect of Gal-SMEDDS was better than that of free Gal. In vivo pharmacokinetic experiments showed that the pharmacokinetic parameters of Gal-SMEDDS were better than that of free Gal, which indicated that the self-microemulsion drug delivery system(SMEDDS) effectively increases the oral bioavailability of Gal and alters its pharmacokinetic parameters, such that it may be effective in the treatment of anti-oxidant.

Keywords: galangin; Self microemulsion drug delivery system; Antioxidant damage; Pharmacokinetics

1. Introduction

Galangin (3,5,7-trihydroxyflavone) is a natural active flavonoid compound, separated from the dried roots and rhizomes of Alpinia ofcinarum Hance[1], a plant of the ginger family, and it also has a higher content in honey, propolis and golden spirulina[2]. Galangin(Gal) is one of the main active components of Alpinia ofcinarum Hance. Modern pharmacological studies have shown that Gal has a variety of biological activities such as anti-tumor[3],[4],[5], anti-fungal[6], anti-bacterial[7],[8], anti-inflammatory[9],[10],[11], anti-ischemic stroke[12], suppressing vitiligo[13] and Alzheimer's disease[14], etc[15],[16]. Recently, there have been reports that Gal has the activity of scavenging oxygen free radicals[17],[18] and shows excellent anti-oxidant effects. Although Gal has rich pharmacological activities and research prospects, the product development of Gal has some application difficulties: one is that it is insoluble in water and sensitive to factors such as temperature, light, and pH[19], the other is that it has poor ability to pass the gastrointestinal barrier when administered orally, which limit its clinical application value. Therefore, the use of modern pharmacy methods to modify the dosage form of Gal to improve its bioavailability has an important role in promoting its clinical application and product development.

In the past decades, pharmaceutical researchers have been working on improving the solubility of poorly soluble drugs by many nanotechnological solutions[20]. The SMEDDS, as a very promising nanoformulation, has the advantages of improving drug targeting, bioavailability, and drug pharmacokinetic properties[21]. Specifically, SMEDDS is an isotropic and thermodynamically stable system composed of drug, natural or synthetic oil phases, emulsifiers, and co-emulsifiers. After oral administration, it can spontaneously form O/W microemulsions with a particle size of 10-100nm under gastrointestinal peristalsis[22]. The formed microemulsions can significantly improve the solubility and oral bioavailability of poorly soluble drugs due to their small particle size

and large specific surface area. Because of the above advantages, it has received more attention in the development of oral preparations[23].

Therefore, in this study, we first prepared a Gal-SMEDDS, and then further evaluated the effect of free Gal and Gal-SMEDDS on the pharmacokinetic parameters of SD rats and the protective effect of oxidative damage on human embryonic lung fibroblasts (HFL1) cells in vitro.

2. Results

2.1. Drawing of Pseudo-Ternary Phase Diagram

Cremophor CO 40 and PEG-400 were mixed in a mass ratio from 1:9 to 9:1.Then the mixed emulsifier was mixed with ethyl oleate in a mass ratio from 9:1 to 5:5 to obtain the blank SMEDDS. 1g SMEDDS with different proportions mentioned above was weighed and mixed in a magnetic stirrer (100 $r \cdot min^{-1}$), and then slowly added 100mL deionized water. The respective mass ratio of the ethyl oleate, Cremophor CO 40, and PEG-400 were recorded when forming the microemulsions. The pseudo-ternary phase diagram was drawn by Origin 9.1 software. As shown in Figure 1, in the microemulsion region, the proportion of ethyl oleate, Cremophor CO 40, and PEG-400 were 10%～40%、25%～80% and 5%～60%, respectively.

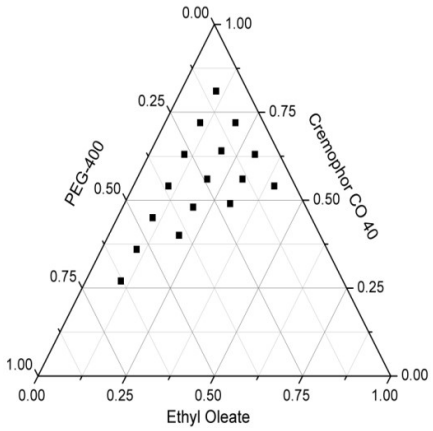

Figure 1 Pseudo-ternary phase diagram of oil phase, emulsifier and emulsifier in Gal-SMEDDS

2.2. Optimization of Gal-SMEDDS formulation by Simplex Lattice Design

Referring to the result of pseudo-ternary phase diagram and the characteristics of each phase, the mass ratio of each component was determined as follows: ethyl oleate (A) is 10%~40%, Cremophor CO 40(B) is 30%~60%, and PEG-400(C) is 30%~60%. Based on this proportion, the average particle size (Y1), polydispersity index (PDI) (Y2), and drug loading (Y3) were chosen as evaluation indexes, and the formulation of simplex grid method was designed by SLD in design expert 10.0.7.0. The specific mass ratio and evaluation results of each Gal-SMEDDS are shown in Table 1.

Table 1. Design and results of simplex grid method for Gal-SMEDDS prescription

NO.	A/%	B/%	C/%	Y_1/(nm）	Y_2(%）	Y_3/(mg/g)
1	10	30	60	33.87	0.168	13.73
2	15	50	35	29.15	0.148	11.71
3	10	60	30	21.04	0.096	21.04
4	40	30	30	182.37	0.225	20.97
5	15	35	40	80.98	0.201	14.37
6	20	40	40	79.81	0.23	10.45
7	25	45	30	56.93	0.245	10.7
8	30	35	35	138.14	0.25	13.83
9	40	30	30	181.43	0.247	20.09
10	10	45	45	25.13	0.119	17.72

11	25	30	45	196.57	0.25	22.76
12	10	60	30	21.82	0.095	20.98
13	25	45	30	57.45	0.242	10.72
14	10	30	60	32.62	0.165	13.67

2.3. Mathematical model fitting and variance analysis

Design Expert 10.0.7.0 software was used to fit the data in Table 1 with the multiple regression model, and the response equation of each index was obtained: Y_1= -15.68365A - 1.61872B - 7.14913C + 0.36462AB + 0.95778AC + 0.17863BC - 0.018768ABC（r=0.9998，r_{adj}=0.9997）；Y_2= -7.08296×10^{-3}A + 3.06837×10^{-4}B + 3.96818×10^{-4} C + 1.84966×10^{-4}AB + 6.89353×10^{-5}AC - 1.09630×10^{-4}BC + 5.11937×10^{-6}ABC（r=0.9825，r_{adj}=0.9675）；Y_3= -4.55377A - 0.74393B - 1.68472C + 0.15378AB + 0.22403AC + 0.067455BC - 6.62669×10^{-3} ABC（r=0.9937，r_{adj}=0.9882）. The variance analysis of the above mathematical model was shown in Table 2. The P value of each response model was less than 0.0001, which indicated that each index response model has reached a very significant level. The P values of the lack of fit were 0.0729, 0.1099, and 0.3919, respectively, which were all greater than 0.05, and the coefficients of regression equation r and the coefficient of correction regression equation r_{adj} of each model were greater than 0.95, which indicated that the regression model fitting was successful and representative, and can predict the optimal prescription.

Table 2 Gal-SMEDDS prescription optimization analysis of variance

Source	df	Y_1			Y_2			Y_3		
		Mean square	F	P	Mean square	F	P	Mean square	F	P
Model	6	55578.71	7563.11	<0.0001	0.044	65.52	<0.0001	261.63	183.11	<0.0001
AB	1	2677.11	2185.79	<0.0001	7.793×10^{-3}	69.50	<0.0001	137.83	578.77	<0.0001
AC	1	6556.26	5353.02	<0.0001	2.083×10^{-3}	18.58	0.0035	26.78	112.44	<0.0001
BC	1	3.45	2.82	0.1372	1.437×10^{-4}	1.28	0.2949	0.059	0.25	0.6329
ABC	1	277.91	226.91	<0.0001	2.068×10^{-5}	0.18	0.6805	34.65	145.29	<0.0001
Residual	7	8.57			7.849×10^{-4}			1.67		
Lack of fit	3	6.91			5.334×10^{-4}			1.28		
Pure error	4	1.66	5.54	0.0658	2.515×10^{-4}	2.83	0.1705	0.39	4.35	0.0947
Cor total	13	55587.28			0.045			263.30		

2.4. Optimization of prescription by Response Surface Methodology

According to the results of regression analysis, two-dimensional contour curve and three-dimensional response surface curve of each factor were drawed, and the results were shown in Figure 2. Figure 2A shows that the average particle size decreased with the increase of the proportion of Cremophor CO 40, and increased with the increase of the proportion of ethyl oleate, while PEG-400 had no significant effect on the average particle size. Figure 2B shows that PDI increased with the increase of the proportion of ethyl oleate, and decreased with the increase of the proportion of Cremophor CO 40 and PEG-400. Figure 2C shows that the drug loading increased with the increase of the proportion of ethyl oleate and Cremophor CO 40, and increased first and then decreased with the increase of the proportion of PEG-400.

The smaller the average particle size, the larger the specific surface area and the narrower the particle size distribution, which means the faster drug dissolution[24]. The higher the drug loading and the smaller the single dose, which means more conducive to clinical application. Considering the above factors and experimental results, the software predicted that the optimal prescription was W (ethyl oleate) : W (Cremophor CO 40): W (PEG-400) = 10%: 60%: 30%, and the average particle size, PDI, and drug loading were 21.376 nm, 0.093, and 20.897 mg/g, respectively. Three batches of Gal-SMEDDS were prepared according to the software prediction, and the average particle size, PDI, and drug loading were determined to be (21.33±0.62) nm, 0.096±0.003, (21.15±0.32) mg/g, respectively. The deviation between the measured value of each index and the predicted value was small, indicating that the established mathematical model has good predictability.

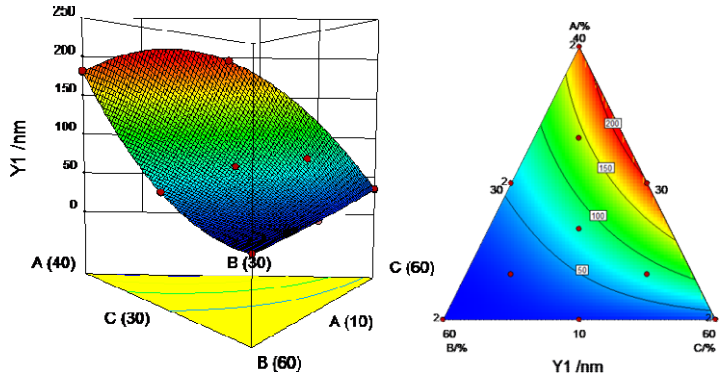

A

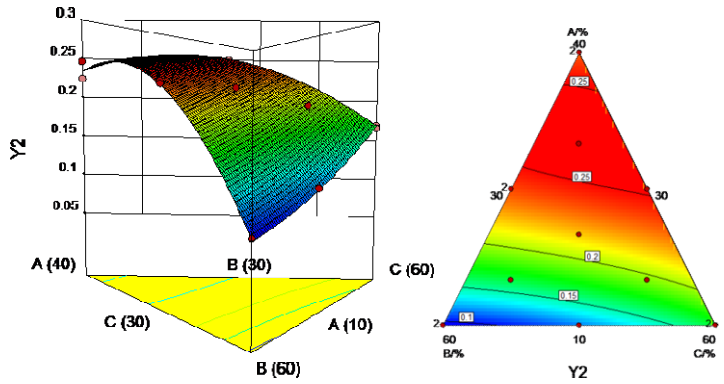

B

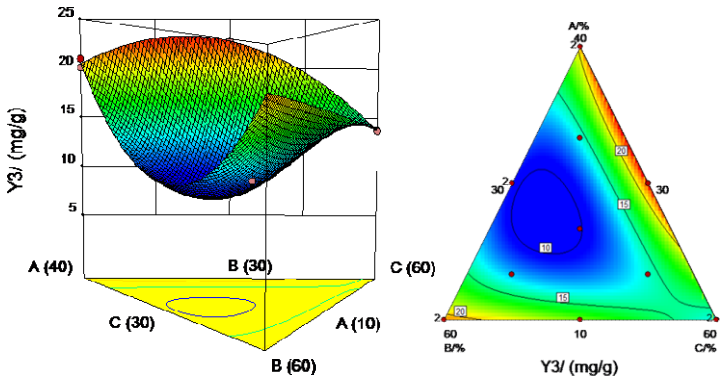

C

A. Average particle size B. PDI C. drug loading

Figure 2 Three dimensional response surface curve, two-dimensional contour curve

2.5. Preparation of Gal-SMEDDS

In summary, the preparation process of Gal-SMEDDS was as follows: According to the mass ratio W (ethyl oleate) : W (Cremophor CO 40) : W (PEG-400)= 10% : 60% : 30%, each component were precisely weighed and placed in a beaker, and ultrasonic treated for 40 min to make them thoroughly mixed, then stirred in a magnetic stirrer (100 r/min) for 15 min to obtain blank SMEDDS. Gal was added to the blank SMEDDS at a drug loading of 20 mg/g and mixed with ultrasound for 40 min. Gal-SMEDDS was obtained by standing at 37 ℃ for 24 h.

2.6. Characterization of Gal-SMEDDS

The morphology of Gal-SMEDDS was observed according to the method in item 2.3. As shown in Figure 3, the microemulsions have a round spherical shape with a size within 100 nm. A Malvern Nano ZS90 was used to measure its average particle size, PDI, and zeta potential according to the method in item 2.4. As shown in Figure 4, the average particle size, PDI, and Zeta potential of the microemulsions were (21.33±0.62) nm, 0.096±0.003, (-4.09±0.11) mV, respectively, with smaller particle size and narrow distribution.

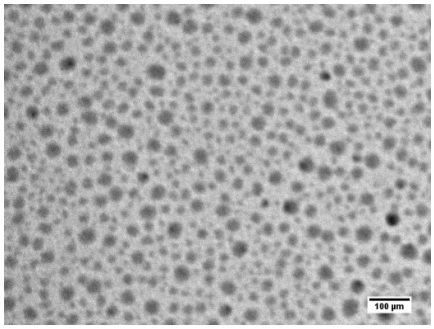

Figure 3 TEM observation images of Gal-SMEDDS (× 30000)

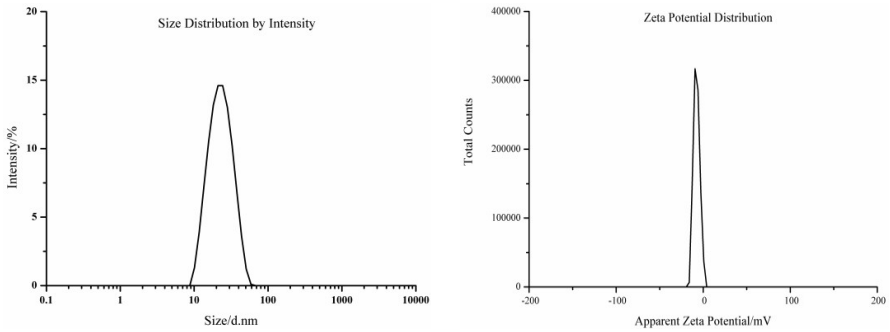

A.Size (d.nm) B. Apparent zeta potential (mV)

Figure 4 particle size distribution and apparent zeta potential of Gal-SMEDDS

2.7. Drug loading and encapsulation efficiency

The drug loading and encapsulation efficiency of Gal-SMEDDS were calculated according to the method in item 2.6. The results showed Gal-SMEDDS has a drug loading capacity of (21.15±0.32) mg/g and an encapsulation efficiency of (96.74±0.25)%.

2.8. In Vitro Release Study

The release profiles of Gal in vitro were summarized according to the method in item 2.7. As shown in Figure 5, the cumulative release of Gal-SMEDDS was significantly higher than that of free Gal in different release media. When released in vitro for 24h, the cumulative release of Gal-SMEDDS and free Gal in deionized water were (87.31±2.52)% and (50.27±1.49)%, respectively; in artificial gastric juice, the cumulative release of Gal-SMEDDS and Gal were (79.37±2.49)% and (39.57±1.29)%, respectively . In artificial intestinal fluid, the cumulative release of Gal-SMEDDS and Gal were (84.14±3.10)% and (45.39±1.28)%, respectively. It showed that SMEDDS can significantly improve the in vitro release of Gal.

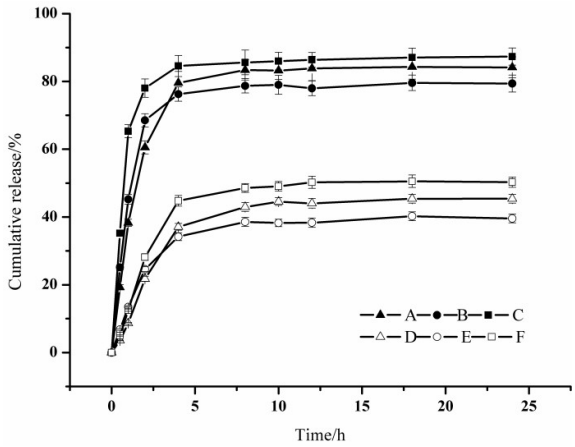

A.Gal-SMEDDS(pH=6.8) B.Gal-SMEDDS(pH=1.2) C.Gal-SMEDDS (deionized water)

D.Gal (pH=6.8) E.Gal (pH=1.2) F.Gal (deionized water)

Figure 5 in vitro release curves of Gal and Gal-SMEDDS in different media

2.9 The effects of Gal on HFL1 viability

The CCK-8 kit was used to detect the cytotoxicity of Gal and H_2O_2 on HFL1 cells, and the results were shown in Figure 6. The results showed that when the concentration of Gal and Gal-SMEDDS was higher than 16μg· mL^{-1}, it had an inhibitory effect on cell survival. When the concentration was in the range of 1-12

μg· mL^{-1}, HFL1 cells had no obvious cytotoxicity, and the cell survival rate was basically the same. Therefore, 1, 6, 12 μg· mL^{-1} were selected as the concentration for subsequent experiments.

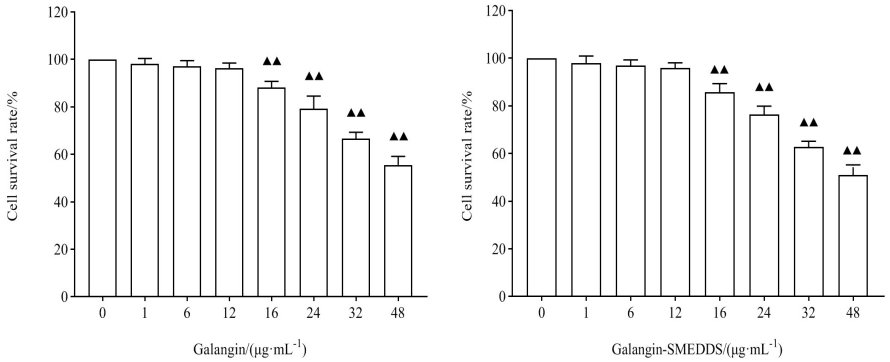

Figure 6 Effects of different concentrations of Gal(A) and Gal-SMEDDS(B) on the viability of HFL1 cells
Compared with the control group, ▲P<0.05, ▲▲P<0.01

2.10 The effects of H_2O_2 on HFL1 viability

The cytotoxicity results of H_2O_2 are shown in Figure 7. The results showed that when the concentration of H_2O_2 was in the range of 500-700 μmol· L^{-1}, the cell survival rate was significantly decreased ($P < 0.05$), and the inhibitory effect was dose-dependent with the concentration of H_2O_2. GraphPad Prism 8.0 software was used to fit the relationship between the concentration of H_2O_2 and cell survival. The results showed that the IC_{50} value of H_2O_2 to HFL1 cells was 525 μmol· L^{-1}, so this concentration was chosen as the modeling concentration.

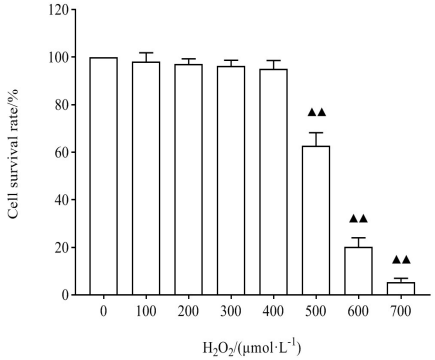

Figure 7 Effects of different concentrations of H_2O_2 on the viability of HFL1 cells
Compared with the control group, ▲▲P<0.05, ▲▲P<0.01

2.11 Effects of Gal on HFL1 viability induced by H_2O_2

The effect of Gal on the viability of HFL1 cells induced by H_2O_2 was shown in Figure 8. The results showed that compared with the control group, the viability of HFL1 cells treated with H_2O_2 was obviously inhibited ($P < 0.05$). Compared with the model group, the viability of cells which pretreated with Gal and Gal-SMEDDS were significantly increased ($P < 0.05$). It showed that both free Gal and Gal-SMEDDS can inhibit the oxidative damage of HFL1 cells induced by H_2O_2, and the Gal-SMEDDS had a more obvious preprotection effect than free Gal ($P < 0.05$).

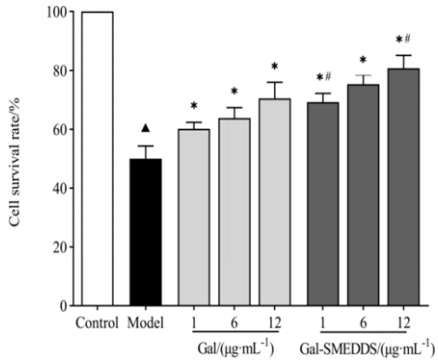

Figure 8 Effect of Gal and Gal-SMEDDS on HFL1 cells viability induced by H_2O_2

(Compared with the control group, ▲P<0.05; compared with the model group, *P<0.05; compared with the Gal group, #P<0.05)

2.12. HFL1 cell apoptosis analysis

The effect of Gal on the apoptosis of HFL1 cells induced by H_2O_2 was shown in Figure 9 and Figure 10. The results showed that the apoptosis rate of HFL1 cells in the model group was 43.10%, while the apoptosis rates of Gal group were 35.20%, 31.80% and 19.70%, respectively, and those of Gal-SMEDDS group were 25.76%, 21.22% and 16.04%, respectively. The apoptosis rate of Gal group and Gal-SMEDDS group were lower than that of the model group (P < 0.05). These results indicated that free Gal and Gal-SMEDDS can significantly reduce the apoptosis rate of HFL1 cells, and the effect of Gal-SMEDDS was more obvious than that of free Gal.

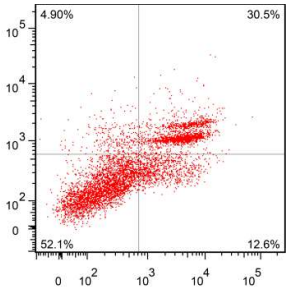

A

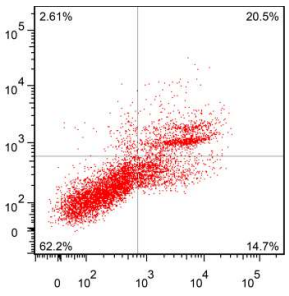

B

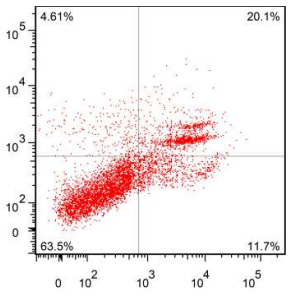

C

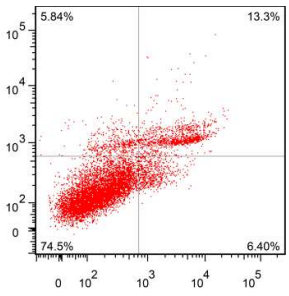

D

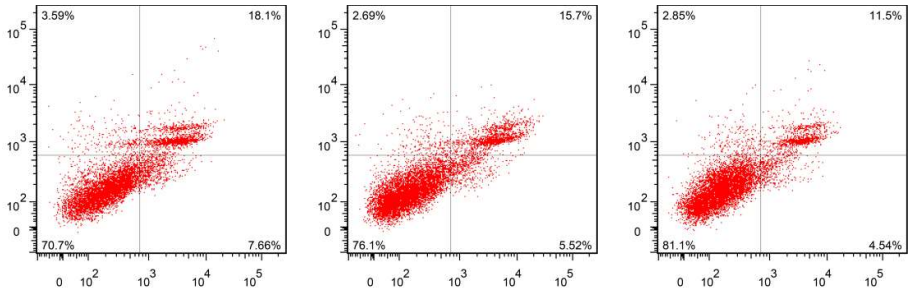

E F G

A. Model group B. Gal low dose group C. Gal medium dose group D. Gal high dose group E. Gal-SMEDDS low dose group F. Gal-SMEDDS medium dose group G. Gal-SMEDDS high dose group

Figure 9. Flow cytometry apoptosis of HFL1 cells in groups

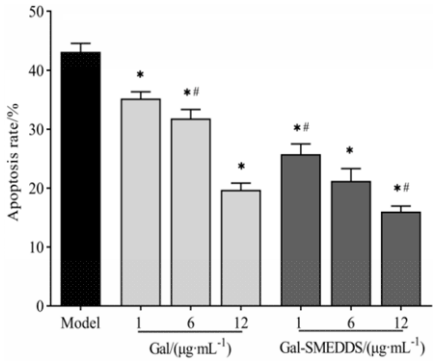

Figure 10. Effect of Gal and Gal-SMEDDS on apoptosis of HFL1 cells

(Compared with the control group, ▲P<0.05; compared with the model group, $^{*}P$<0.05; compared with the Gal group, $^{\#}P$<0.05)

2.13 Detection of ROS level in HFL1 cells

ROS fluorescence kit was used to detect the level of ROS in HFL1 cells induced by H_2O_2. The excitation wavelength of fluorescence was 502 nm, the emission wavelength was 530 nm, and the FITC fluorescence intensity was proportional to the level of ROS in the cell. As it was shown in Figure 11, compared with the control group, the intracellular FITC fluorescence intensity of HFL1 cells treated with H_2O_2 increased significantly, which indicated that H_2O_2 can induce HFL1 cells release large amounts of ROS. Compared with the model group, the intracellular FITC fluorescence intensity of HFL1 cells decreased after the intervention of Gal and Gal-SMEDDS(P<0.05). The results showed that both free Gal and Gal-SMEDDS can inhibit the release of ROS induced by H_2O_2, and the effect of Gal-SMEDDS was more obvious than that of free Gal.

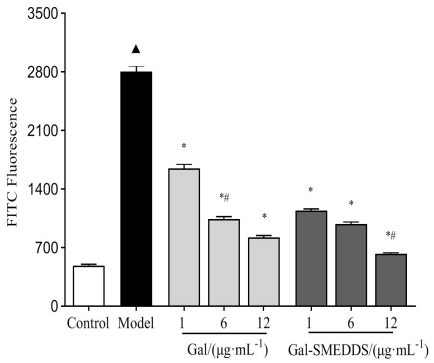

Figure 11. Effect of Gal and Gal-SMEDDS on ROS level in HFL1 cells

(Compared with the control group, ▲P<0.05; compared with the model group, *P<0.05; compared with the Gal group, #P<0.05)

2.14 Pharmacokinetic parameters

According to the method in item 2.14, the samples were prepared at each time point and analyzed by HPLC. The concentration of Gal was calculated and the plasma concentration-time curves of the two groups were drawn. As it was shown in Figure 12, the absorption degree and speed of Gal-SMEDDS in rats were higher than that of free Gal. DAS 2.1.1 software was used to process the data and showed that both free Gal and Gal-SMEDDS were two-compartment open models. Statistical moment method was used to calculate the pharmacokinetic parameters of the two groups, and the statistical t-test was performed. As it was shown in Table 3, the C_{max}, $AUC_{0\text{-}24h}$, $AUC_{0\text{-}\infty h}$ and MRT of Gal-SMEDDS group were significantly increased, which were 1.74 times, 1.71 times, 1.80 times and 1.23 times of Gal group respectively. The results indicated that compared with free Gal, Gal-SMEDDS had the advantages of rapid absorption, sufficient absorption, delayed drug release, and can significantly improve the oral bioavailability of free Gal.

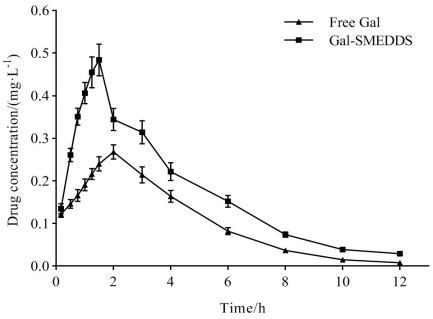

Figure 12. Plasma concentration-time curve of Gal and Gal-SMEDDS in rats at 0-12h after ig administration

Table 3. Pharmacokinetic parameters after oral administration free Gal and Gal-SMEDDS in rats

Parameters	free Gal	Gal-SMEDDS
$t_{1/2\alpha}$ (h)	1.547 ± 0.108	1.813 ± 0.069#

$t_{1/2\beta}$ (h)	1.646 ± 0.132	3.265 ± 0.300#
T_{max} (h)	1.789 ± 0.074	1.411 ± 0.069#
C_{max} (mg·L^{-1})	0.245 ± 0.016	0.427 ± 0.034#
AUC_{0-24h} (mg·h·L^{-1})	1.207 ± 0.088	2.059 ± 0.176#
$AUC_{0-\infty h}$ (mg·h·L^{-1})	1.224 ± 0.091	2.202 ± 0.512#
AUMC (mg·h^2·L^{-1})	4.537 ± 0.252	10.000 ± 0.461#
MRT (h)	3.708 ± 0.146	4.542 ± 0.192#

#P<0.05 vs free Gal group

3. Discussion

As a flavonoid, Gal has a variety of pharmacological activities, such as anti-inflammatory, anti-tumor, anti-oxidation, anti-bacterial. However, it is insoluble in water and sensitive to light and pH, resulting in low oral bioavailability and difficulty in product development and application. Therefore, we used modern pharmacy methods to modify its dosage form and prepared the Gal-SMEDDS[25]. First, by drawing a pseudo-ternary phase diagram, the proportions of the ethyl oleate, Cremophor CO 40, and PEG-400 in Gal-SMEDDS were determined; on the basis of this proportion, the average particle size, PDI and drug loading were taken as the indexes to optimize and determine the formulation of Gal-SMEDDS by simplex grid method, which is an experimental method that can accurately predict the performance of other points in the experimental area with a less times of experiments, and is widely used in the optimization of drug prescription. The prepared Gal-SMEDDS was a light yellow transparent liquid without stratification and insoluble components. It had small average particle size (21.33nm), narrow distribution(PDI 0.096), high drug loading (20.03±0.21mg·g^{-1}) , and good encapsulation efficiency (96.74±0.25%).

Then we evaluated the in vitro release of the prepared Gal-SMEDDS. In order to better simulate the pH environment of the body, artificial gastric juice, artificial intestinal juice, and deionized water were used as dissolution media. The results showed that the cumulative release rates of Gal and Gal-SMEDDS in deionized water, artificial intestinal juice, and artificial gastric juice decreased in turn. The reason may be that with the increase of pH value of the release medium, the hydrogen bond between water molecule and Gal was strengthened, which promoted the release of Gal. The cumulative release rate of Gal in Gal-SMEDDS was significantly higher than that of free Gal in different release media, which indicated that SMEDDS had the potential to increase the gastrointestinal absorption rate of Gal and improve the bioavailability of Gal. The reason may be due to the microemulsions formed under mild stirring conditions and the microemulsions had small particle size and large specific surface area, which can help the dissolution of Gal in the medium and accelerate the release of Gal. In addition, Cremophor CO 40, an emulsifier in the formulation, can also improve the drug release rate by increasing the solubility of Gal.

After the preparation of Gal-SMEDDS, the antioxidant capacities of Gal and Gal-SMEDDS were investigated by cell experiment in vitro. In the normal physiological state, the body is in a dynamic balance of oxidation and antioxidation. A small amount of ROS produced in the body can be eliminated by the antioxidant defense system. When the accumulation rate of ROS exceeds the elimination rate of the body itself, the dynamic balance of oxidation/antioxidant will be unbalanced, which can lead to many diseases, such as pulmonary fibrosis, Parkinson's disease, Alzheimer's disease and cerebral ischemia[26]. Therefore antioxidation plays an important role in the prevention of these diseases. Our experimental study found that 525 μmol·L^{-1} H_2O_2 treated HFL1 cells for 24 h can successfully prepare HFL1 cells oxidative damage model. Gal and Gal-SMEDDS can inhibit cell oxidative damage by reducing ROS level and apoptosis rate, and the antioxidant effect of Gal-SMEDDS was better than that of Gal.

Finally, we compared the pharmacokinetics of the prepared Gal-SMEDDS and the free Gal. The results of pharmacokinetic studies showed that free Gal and Gal-SMEDDS were both two-compartment open models, which indicated that the elimination process of the two in rats was similar, and the difference in absorption may be related to the form of the preparation. The difference between Gal and Gal-SMEDDS in C_{max}, $AU_{C0\text{-}24h}$, $AUC_{0\text{-}\infty h}$, and MRT was statistically significant (P <0.05), and Gal-SMEDDS had better effect on promoting absorption. Based on references[27,28], we speculated that the reason may be that Gal-SMEDDS forms microemulsions under the peristalsis of the physiological functions of the gastrointestinal tract. The small size of the microemulsions was beneficial to the absorption of Gal and can also reduce the enzymatic hydrolysis of Gal in the gastrointestinal tract. In addition, ethyl oleate and Cremophor CO 40 can increase the net absorption of Gal in intestinal epithelial cells and improve the bioavailability of galangin by increasing the cell bypass transport of Gal, enhancing the permeability of cell membrane to Gal, and inhibiting its P-gp efflux.

4. Materials and Methods

4.1. Materials

Gal with the purity of 99% was provided by Aladdin Co. Ltd (Shanghai, China). ethyl oleate and PEG-400 were purchased from Ruisheng Pharmaceutical Excipients Co. Ltd (Shandong, China). Cremophor CO 40 was bought from Yousuo Chemical Technology Co. Ltd (Shandong, China). Acetonitrile and methanol were purchased from Thermo Fisher Scientific (Waltham, MA). Hydrogen peroxide(H_2O_2) was bought from Damao Chemical Reagent Factory (Tianjin, China). HFL1 cells were purchased from Qishi Co. Ltd (Jiangshu, China). F-12k medium was bought from Jinuo Co. Ltd (Zhengjiang, China). Cell Counting Kit-8 (CCK-8) was bought from biosharp Biotech (Hefei, China). Annexin V-FITC/PI Apoptosis Detection Kit was bought from Beibo Co.Ltd (Shanghai, China). Reactive Oxygen Species (ROS) Assay Kit was bought from Elabscience Co. Ltd (Wuhan, China). Male Sprague Dawley rats were purchased from Changsheng Co. Ltd (Shenyang, China).

4.2. Preparation of Gal-SMEDDS

Ethyl oleate, Cremophor CO 40, and PEG-400 were selected as the oil phase, emulsifier and co emulsifier. Gal-SMEDDS was prepared by the following methods： ethyl oleate, Cremophor CO 40, and PEG-400 were precisely weighed and placed in a beaker, and ultrasonic treated for 40 min to make them thoroughly mixed, and then stirred in a magnetic stirrer (100 r/min) for 15 min to obtain a blank SMEDDS. Gal was added to the blank SMEDDS at a drug loading of 20 mg/g and mixed with ultrasound for 40 min. Gal-SMEDDS was obtained by standing at 37 ℃ for 24 h.

4.3. Transmission Electron Microscopy

Phosphotungstic acid negative staining method was used to observe the morphology of Gal-SMEDDS. Gal-SMEDDS was diluted to 100 times with deionized water and mixed with the same amount of 2% phosphotungstic acid for 3 min. The mixed liquid was dropped on a film-coated copper grid and stained for 10 min and then filter paper was used to absorb the excess dye solution. The morphology of the microemulsions was observed under a transmission electron microscope (TEM, JEM-1400, JEOL, Japan).

4.4. Particle Size and Zeta Potential Measurement

Gal-SMEDDS was diluted to 100 times with deionized water, and its average particle size, PDI, and Zeta potential were measured by a dynamic light scattering method using the Malvern Nano ZS90 (Malvern, UK). Raw data were collected at 25℃ at an angle of 90° , each measurement being performed in triplicate.

4.5. Determination of Gal Concentration

HPLC (LC-20AT, Shimadzu, Japan) was used to quantitative the concentration of Gal with a C18 column (4.6 mm × 250 mm, 5 μm, inertstain) at at the column temperature of 35°C and the wavelength of 266nm. The mobile phase was a mixture of methanol and 0.2% phosphoric acid (68:32, V/V) at a flow rate of 1 mL /min. The sample was diluted with methanol and the injection volume was 10 μL.

4.6. Measurement of encapsulation efficiency and drug loading

0.25 g Gal-SMEDDS was precisely weighed and recorded as W_1, and it was added in a 25 mL capacity bottle, diluted with deionized water to the scale mark, and shaked to form the microemulsions. 4 mL microemulsions was added in a centrifuge tube and centrifuged for 15min at 10000 r/min. 0.25 mL supernatant was added in a 25 mL volumetric flask and diluted with methanol to the scale mark and analyzed for Gal. The concentration of Gal was measured according to the chromatographic conditions in item 2.5. The content of Gal was calculated based on its concentration and recorded it as W_2.

Similarly, 0.25 g Gal-SMEDDS was precisely weighed and recorded as W_3, and it was added in a 25 mL capacity bottle, diluted with methanol to the scale mark, and analyzed for Gal. The content of Gal was calculated and recorded as W_4.

Entrapment efficiency (EE%) was quantified using the following equation: $EE\% = W_2/W_1 \times 100\%$. Drug loading (DL%) was quantified using the following equation: $DL\% = W_4/W_3 \times 100\%$.

4.7. In Vitro Release Study

Dynamic dialysis method[29] was used to determine the in vitro release of free Gal and Gal-SMEDDS in pH=1.2 artificial gastric juice, pH=6.8 artificial intestinal juice and deionized water. Briefly, free Gal and Gal-SMEDDS were transferred into pretreated MD44 dialysis bags (molecular retention is 8000-14000 KD). The dialysis bag was tightened and immersed into a beaker containing 500mL release medium, respectively. The beakers were placed in a constant temperature water bath shaker (37°C, 100rpm). The samples of 2 mL were taked at 0.5, 1, 2, 4, 8, 10, 12, 16, and 24 h and supplemented with an equal volume of fresh dialysis medium. The samples were passed through a 0.45 μm microporous filter membrane. The subsequent filtrates were used as the test product for HPLC and the concentration and cumulative release rate were calculated based on the HPLC results.

4.8. Cell culture

HFL1 cells were cultured in F-12K medium (Kaighn's Modification of Ham's F-12 Medium) and incubated at 37℃ in a humidified 5% CO_2 atmosphere. HFL1 cells in the logarithmic growth phase were used for cell viability, apoptosis, and ROS detection.

4.9. Cell viability

The cells were adjusted to 1×10^5 cells / mL and seeded into 96-well plates according to 100 μL per well and cultured in F-12k medium containing different concentrations of Gal (1, 6, 12, 16， 24, 32, 48 μg· mL^{-1}) in a humidifed 5% CO_2 atmosphere at 37 ℃ for 24h. Discarding the cell culture medium, 100 μL of F-12k medium containing 10% CCK8 was added to each well and cultured for 4 h. After that, the absorbance (OD) value at 450 nm was detected in a Model 680 microplate reader((Bio-Rad, Hercules, CA, USA). Referring to the above experimental procedure, the HFL1 cells were treated with different concentrations of H_2O_2 (100, 200, 300, 400, 500, 600, 700 μmol· L^{-1}). The concentration of H_2O_2 with 50% cell survival rate was selected as the model concentration of HFL1 cell oxidative damage.

4.10. Effects of Gal on HFL1 cell damage caused by H_2O_2

The cells were adjusted to 2×10^5 cells / mL and seeded into 6-well plates according to 1000 μL per well and pre-cultured in F-12k medium containing free Gal and Gal-SMEDDS (1,6,12 μg· mL^{-1}) for 24 h. Then 525 μmol· L^{-1} H_2O_2 solution was added and treated for 24 h. Discarding the cell culture medium, 100 μL of f-12k medium containing 10% CCK8 was added to each well and cultured for 4 h. After that, the OD value at 450nm was detected in a Model 680 microplate reader. Untreated cells were considered as the control group and the model group cells were only treated with 525 μmol· L^{-1} H_2O_2..

4.11. HFL1 cell apoptosis detection

The Annexin V-FITC/7-AAD double staining cell apoptosis detection kit was used to detect the effects of free Gal and Gal-SMEDDS on the apoptosis of HFL1 cells. The cells were adjusted to 2×10^5 cells / mL and seeded into 6-well plates according to 1000 μL per well and pre-cultured in F-12k medium containing free Gal and Gal-SMEDDS (1,6,12 μg· mL^{-1}) for 24 h. Then 525 μmol· L^{-1} H_2O_2 solution was added and treated for 24 h. The cell culture medium of each group was collected and mixed with the digested cell suspension, and then centrifuged at 5 000 r·min^{-1} for 5 min to collect the precipitated cells. Washing Cells twice with PBS at 4℃, resuspending the cells with Annexin V binding solution to adjust the density to 1×10^6 cells·mL^{-1}. Annexin V-FITC staining solution was added to the collected cells and incubated at 2-8℃ for 15 min, and 7-AAD staining solution was added for 5 min at 2-8℃. Finally, the blank tube and two single staining tubes were adjusted to compensate the voltage, and the apoptosis rate was detected by flow cytometry. The model group cells were only treated with 525 μmol· L^{-1} H_2O_2.

4.12. Detection of ROS level in HFL1 cells

The ROS fluorescence assay kit was used to detect the effects of free Gal and Gal-SMEDDS on the ROS level of HFL1 cells. The cells were adjusted to 2×10^5 cells / mL and seeded into 6-well plates according to 1000 μL per well and pre-cultured in F-12k medium containing free Gal and Gal-SMEDDS (1,6,12 μg· mL^{-1}) for 24 h. Then 525 μmol· L^{-1} H_2O_2 solution was added and treated for 24 h. The supernatant was removed and the cells were digested with 0.25% trypsin for 2-3 min and centrifuged at 3000r· min^{-1} for 10 min. The cells were collected and resuspended, and the ROS level was detected by flow cytometry. Un-

treated cells were considered as the control group and the model group cells were only treated with 525 μmol· L^{-1} H_2O_2..

4.13. In Vivo Pharmacokinetic Analysis

The pharmacokinetic parameters of free Gal and Gal-SMEDDS in rats were compared after intragastric administration at doses of 50 mg·kg^{-1}. The male SPF grade SD rats weighing 240g±20g were raised in the experimental animal center of Hubei University of Chinese Medicine with a standard light (12 h light/dark) and temperature condition (23±2℃) for 1 week. According to the random number table method, the rats were divided into 2 groups, each with 6 rats, and fasted 12 hours before dosing. After 1 week of adaptive breeding, the free Gal and Gal-SMEDDS were intragastrically administered to each group at the dosage of 50 mg·kg^{-1}. At 0.17, 0.5, 0.75, 1, 1.25, 1.5, 2, 3, 4, 6, 8, 10 and 12 hours after administration. 0.5 mL blood was collected from the orbital venous plexus of each rat and placed in a centrifuge tube soaked with heparin sodium, and centrifuged at 5 000r· min^{-1} for 15 min. The plasma supernatant was immediately separated and stored in a frozen state at -20℃until analyzed. DAS 2.1.1 pharmacokinetic software was used to process the average blood drug concentration data. The main pharmacokinetic parameters include maximum concentration (C_{max}), maximum time (T_{max}), area under the curve ($AUC_{0\text{-}24h}$, $AUC_{0\text{-}\infty h}$), biological half-life ($T_{1/2}$), area under the first moment of the plasma concentration-time curve (AUMC) and mean resident time (MRT).

4.14. Statistical Analysis.

The results were expressed as mean± standard deviation (SD) of at least three independent experiments. Statistical significance was tested by one-way analysis of variance (ANOVA) by IBM SPSS Statistics 22.0 software. The data had statistical significance when $p < 0.05$.

5. Conclusions

In conclusion, a self-microemulsion drug delivery system of Gal was prepared, and its release in vitro and pharmacokinetics in vivo were evaluated. The results showed that the self-microemulsion drug delivery system can significantly improve the cumulative release rate in vitro and pharmacokinetic parameters in vivo of free Gal. Cell experiments showed that Gal can protect HFL1 cells from oxidative damage induced by H_2O_2. The mechanism may be related to Gal can reduce the level of ROS, and inhibit cell apoptosis in damaged cells, and the anti-oxidant effect of Gal-SMEDDS was better than that of free Gal. In future research, we will further research the signal transduction pathway of Gal antioxidants and its influence on the expression of apoptosis genes, and carry out in vivo pharmacodynamic research.

Author Contributions: Conceptualization, Hanlin Xu; Data curation, Hao Lu and Hanlin Xu; Formal analysis, Hao Lu; Funding acquisition, Hao Lu; Investigation, Xiwen Chen; Supervision, Hanlin Xu; Validation, Hanlin Xu; Writing – original draft, Xiwen Chen; Writing – review & editing, Hao Lu.

Funding: This research received no external funding

Data Availability Statement: The data used to support the findings of this study are available from the corresponding author upon request.

Conflicts of Interest: The authors declare no conflict of interest.

References

[1] Heo M Y, Sohn S J, Au W W. Anti-genotoxicity of galangin as a cancer chemopreventive agent candidate[J]. Mutat Res, 2001, 488(2):135-150.
[2] Patel D K, Patel K, Gadewar M, et al. Pharmacological and bioanalytical aspects of galangin-a concise report[J]. ASIAN PAC J TROP MED, 2012, 2(1):449-455.
[3] Chen D L, Li D F, Xu X B, et al. Galangin inhibits epithelial-mesenchymal transition and angiogenesis by downregulating CD44 in glioma[J]. J CANCER, 2019, 10(19):4499-4508.
[4] Yu S, Gong L S, Li N F, et al. Galangin (GG) combined with cisplatin (DDP) to suppress human lung cancer by inhibition of STAT3-regulated NF-κB and Bcl-2/Bax signaling pathways[J]. BIOMED PHARMACOTHER, 2018, 97:213-224.
[5] Wang Y J, Lin B Y, Li H M, et al. Galangin suppresses hepatocellular carcinoma cell proliferation by reversing the Warburg effect[J]. BIOMED PHARMACOTHER, 2017, 95:1295-1300.
[6] Chudapongse N , Klahan K , Kamkhunthod M , et al. Antifungal activity against Candida albicans and effect on mitochondrial NADH oxidation of galangin[J]. PLANTA MED, 2010, 76(12):415.
[7] Ouyang J, Sun F, Feng W, et al. Antimicrobial Activity of Galangin and Its Effects on Murein Hydrolases of Vancomycin-Intermediate Staphylococcus aureus (VISA) Strain Mu50[J]. CHEMOTHERAPY, 2018, 63(1):20-28.
[8] Eumkeb G, Sakdarat S, Siriwong S. Reversing β-lactam antibiotic resistance of Staphylococcus aureus with galangin from Alpinia officinarum Hance and synergism with ceftazidime[J]. PHYTOMEDICINE, 2011, 18(1):40-45.
[9] Wang H B, Hang S H, Xu M, et al. Galangin ameliorates cardiac remodeling via the MEK1/2-ERK1/2 and PI3K-AKT pathways[J]. J CELL PHYSIOL, 2019, 234(9):15654-15667.
[10] Lu H, Yao H, Zou R, et al. Galangin Suppresses Renal Inflammation Via the Inhibition of NF-κB, PI3K/AKT and NLRP3 in Uric Acid Treated NRK-52E Tubular Epithelial Cells[J].
BIOMED RES INT, .2019, 5(26):3018357.
[11] Eun K M, Reum P P, Yong N J, et al. Anti-neuroinflammatory effects of galangin in LPS-stimulated BV-2 microglia through regulation of IL-1β production and the NF-κB signaling pathways[J]. MOL CELL BIOCHEM, 2019, 451(1):145-153.
[12] Wu C , Chen J , Chen C , et al. Wnt/β-catenin coupled with HIF-1α/VEGF signaling pathways involved in galangin neurovascular unit protection from focal cerebral ischemia[J].
SCI REP-UK, 2015, 5:16151.
[13] Huo S X, Liu X M, Ge C H, et al. The Effects of Galangin on a Mouse Model of Vitiligo Induced by Hydroquinone[J]. PHYTOTHER RES, 2014, 28(10):1533-1538.
[14] Zeng H , Huang P , Wang X , et al. Galangin-induced down-regulation of BACE1 by epigenetic mechanisms in SH-SY5Y cells[J]. NEUROSCIENCES, 2015, 294(1):172-181.
[15] Amal A A, Chinnadurai V, Chandramohan G, et al. Galangin controls streptozotocin-caused glucose homeostasis and reverses glycolytic and gluconeogenic enzyme changes in rats[J]. ARCH PHYSIOL BIOCHEM, 2020, 126(2):101-106.
[16] Kim Y J, Lee E H, Cho E B, et al. Protective effects of galangin against UVB irradiation-induced photo-aging in CCD-986sk human skin fibroblasts[J]. APPL BIOL CHEM, 2019, 62(1):40.
[17] Duthie G, Morrice P. Antioxidant Capacity of Flavonoids in Hepatic Microsomes Is not Reflected by Antioxidant Effects In Vivo[J]. OXID MED CELL LONGEV, 2012, 2012(1):1-6.
[18] Kim M E, Park P R, Na J Y, et al. Anti-neuroinflammatory effects of galangin in LPS-stimulated BV-2 microglia through regulation of IL-1β production and the NF-κB signaling pathways[J]. MOL CELL BIOCHEM, 2019, 451(1-2):145-153.
[19] Sulaiman, Mohammad G . Molecular structure and anti-proliferative effect of galangin in HCT-116 cells: In vitro study[J]. FOOD SCI BIOTECHNOL, 2016, 25(1):247-252.
[20] Zhu Y, Wen L M, Li R, et al. Recent advances of nano-drug delivery system in oral squamous cell carcinoma treatment[J]. EUR REV MED PHARMACO, 2019, 23(21):9445-9453.
[21] Yan B B, Ma Y Y, Guo J, et al. Self-microemulsifying delivery system for improving bioavailability of water insoluble drugs[J]. EUR REV MED PHARMACO, 2020, 22(8):374-387.
[22] Mcclements D J. Nanoemulsions versus microemulsions: terminology, differences, and similarities[J]. SOFT MATTER, 2012, 8(6):17194-1729.
[23] Man N, Wang Q L, Li H H, et al. Improved oral bioavailability of myricitrin by liquid self-microemulsifying drug delivery systems[J]. J DRUG DELIV SCI TEC, 2019, 52:597-606.
[24] GALLI C. Experimental determination of the diffusionboundary layer width of micron and submicron particles[J]. INT J PHARMACEUT, 2006, 313 (1-2) :114-122.
[25] Thomas N, Holm R, Garmer M, et al. Supersaturated Self-Nanoemulsifying Drug Delivery Systems (Super-SNEDDS) Enhance the Bioavailability of the Poorly Water-Soluble Drug Simvastatin in Dogs[J]. AAPS J, 2013, 15(1):219-227.
[26] Zhang Z , Yi P , Yi M , et al. Protective Effect of Quercetin against H2O2-Induced Oxidative Damage in PC-12 Cells: Comprehensive Analysis of a lncRNA-Associated ceRNA Network[J]. OXID MED CELL LONGEV, 2020, 2020(2):1-22.
[27] Goo Y T, Song S H, Yeom D W, et al. Enhanced oral bioavailability of valsartan in rats using a supersaturable self-microemulsifying drug delivery system with P-glycoprotein inhibitors[J]. PHARM DEV TECHNOL, 2020, 25(2):178-186.
[28] Liu J , Wang Q L , Emmanuel Q S , et al. Enhanced oral bioavailability of Bisdemethoxycurcumin-loaded self-microemulsifying drug delivery system: Formulation design, in vitro and in vivo evaluation[J]. INT J PHARMACEUT, 2020, 590(1):119887.

[29] Yao H, Lu H, Zhang J, et al. Preparation of Prolonged-Circulating Galangin-Loaded Liposomes and Evaluation of Antitumor Efficacy In Vitro and Pharmacokinetics In Vivo[J]. J NANOMATER, 2019, 2019:1-9.